PLASTIC UPCYCLING

Low-temperature upcycling of polyolefins into liquid alkanes via tandem cracking-alkylation

Wei Zhang[1]*, Sungmin Kim[2], Lennart Wahl[1], Rachit Khare[1], Lillian Hale[2], Jianzhi Hu[2], Donald M. Camaioni[2], Oliver Y. Gutiérrez[2], Yue Liu[1,3]*, Johannes A. Lercher[1,2]*

Selective upcycling of polyolefin waste has been hampered by the relatively high temperatures that are required to cleave the carbon-carbon (C–C) bonds at reasonably high rates. We present a distinctive approach that uses a highly ionic reaction environment to increase the polymer reactivity and lower the energy of ionic transition states. Combining endothermic cleavage of the polymer C–C bonds with exothermic alkylation reactions of the cracking products enables full conversion of polyethylene and polypropylene to liquid isoalkanes (C_6 to C_{10}) at temperatures below 100°C. Both reactions are catalyzed by a Lewis acidic species that is generated in a chloroaluminate ionic liquid. The alkylate product forms a separate phase and is easily separated from the reactant catalyst mixture. The process can convert unprocessed postconsumer items to high-quality liquid alkanes with high yields.

P lastic is ubiquitous in products that range from packaging and textiles to medical equipment and vehicle components (*1*). More than 360 million tonnes per year (estimated 3 to 4% of the total carbon processed per year) of plastic is produced globally, and most of the disposed plastic accumulates in landfills or is dispersed into water bodies (*2, 3*). The chemically inert polyolefins, which amount to more than half of all plastics, are challenging to convert below their melting or softening point (*4*). At the present time, recycling technologies are still dominated by mechanical recycling and thermal conversion (incineration and pyrolysis) (*5, 6*). As a consequence, catalytic upgrading of polyolefin waste into fuels and value-added chemicals has seen substantial research attention, and exciting solutions based on multifunctional catalysts have been emerging (*7*).

Conversion of waste polyolefins is particularly challenging because of the $C(sp^3)$–$C(sp^3)$ bonds, which are more stable than the C-heteroatom bonds of functionalized polymers such as polyesters and polyamides (*8*). Additionally, the endothermic cleavage of the C–C bonds renders processes thermodynamically unfavorable at low temperatures. As a result, converting polyolefins typically requires severe reaction conditions to overcome the kinetic and thermodynamic constraints (*9*). This has been addressed in recent pioneering contributions through the integration of the endothermic C–C cleavage with exothermic reactions—including hydrogenolysis (*10–13*), cross-metathesis (*14, 15*), and aromatization (*16*)—which achieves conversions beyond the equilibria for cracking (fig. S1).

Thermodynamically balancing the exothermic and endothermic kinetically coupled reactions, however, is insufficient to allow for industrially compatible rates below 100°C. The stability of C–C bonds and steric and diffusional barriers that limit the contact of polymer strands with catalytically active sites lead to very slow rates (*17*). As a consequence, most tandem processes require moderate to high reaction temperatures (typically 200° to 250°C) and diverse catalyst functions for relevant conversion rates; these processes lack precise spatiotemporal control over reactive intermediates among catalytic sites (*18*) and complicate product separation and catalyst recovery (*19*). Approaches that would allow selective conversions at substantially lower temperatures would facilitate reactive polymer recycling and open possibilities for decentralized catalytic upgrading.

To achieve this, we turn to coupling cracking of the polymer with alkylation of the formed alkenes by light isoparaffins [isobutane and isopentane (iC_5)]. At present, the refining process is used to produce triple-branched alkanes with a high octane number, which are used in high-octane gasoline (*20*). Conceptually, linking the endothermic
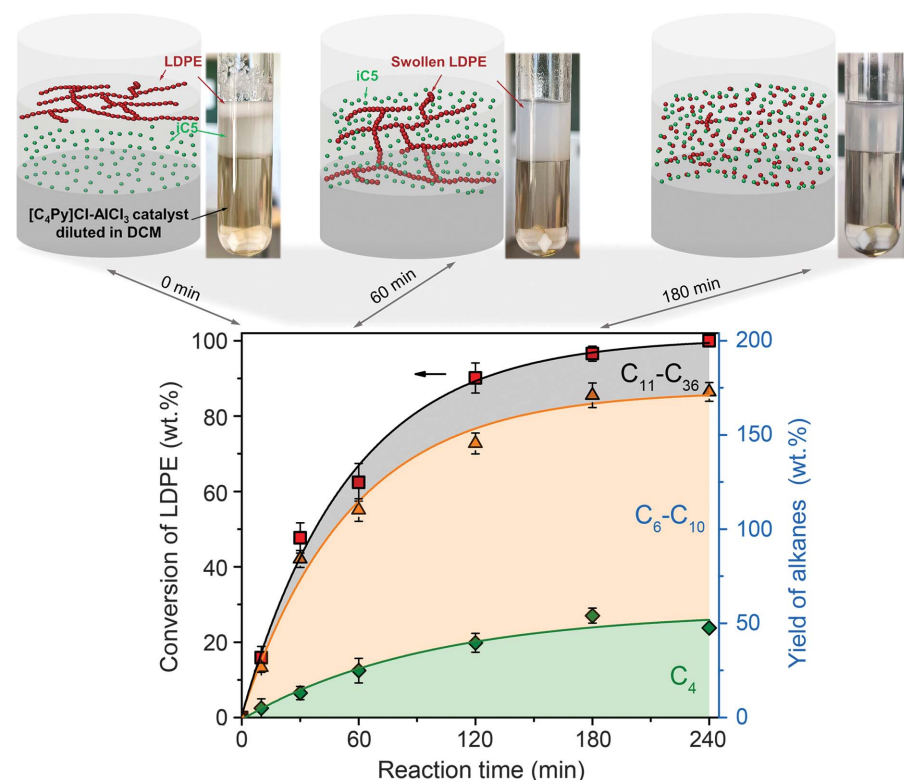

Fig. 1. One-pot catalytic LDPE and *iC*₅ upcycling into liquid alkanes over Lewis acidic chloroaluminate ionic liquid at 70°C. The time-resolved conversion profile of LDPE and cumulative yield of alkanes (C_4, green diamonds; C_6 to C_{10}, orange triangles; C_{11} to C_{36}, red squares) (bottom). Reaction conditions were as follows: LDPE, 200 mg; iC_5, 800 mg; [C₄Py]Cl-AlCl₃ ([C₄Py]Cl:AlCl₃ molar ratio of 1: 2), 3 mmol; TBC as an additive, 0.05 mmol (5 mg); DCM, 3 ml; and temperature, 70°C. The snapshots of the LDPE conversion (top) are at 0, 60, and 180 min from left to right. Curves represent the optimal fit to the data, and all data were repeated at least five times and are shown as mean data points with error bars.

[1]Department of Chemistry and Catalysis Research Center, Technische Universität München, Lichtenbergstr. 4, 85747 Garching, Germany. [2]Institute for Integrated Catalysis, Pacific Northwest National Laboratory, PO Box 999, Richland, WA 99352, USA. [3]Shanghai Key Laboratory of Green Chemistry and Chemical Processes, School of Chemistry and Molecular Engineering, East China Normal University, Shanghai 200062, PR China.
*Corresponding author. Email: w.zhang@tum.de (W.Z.); liuyue@chem.ecnu.edu.cn (Y.L.); johannes.lercher@ch.tum.de (J.A.L.)

cleavage of the polymer C–C bonds to the exothermic alkylation of isoparaffins (i.e., alkylation of the primary alkenes formed from the C–C cleavage by using paraffins whose carbon atoms are retained in the products) couples the two reactions kinetically and, hence, thermodynamically allows full conversion of the polymer below 100°C. All of these reactions are posited to share carbenium ions as intermediates (21), which means that they can operate simultaneously within the same medium and with the same catalyst. We showed recently that a highly polar reaction environment strongly increases the standard chemical potential and reactivity of a nonionic reactant (the polymer in this case) and stabilizes the carbenium ion transition states, thereby lowering the overall free-energy barrier of the coupled reactions and notably enhancing reactivity (22, 23).

Combining the concurrent tandem catalysis of cracking-alkylation and polarity-tailored reactant environments, we report here a strategy for the catalytic upgrading of discarded polyolefins and isoparaffins (recycled from the light end of products formed in the process) into gasoline-range alkanes in a single stage.

The process enables the upcycling of waste polyethylene with full conversion at 70°C to a narrow distribution of branched liquid alkanes (C_6 to C_{10}) on Lewis acidic chloroaluminate ionic liquid [which is being used as the source of the alkylation catalyst species (24)]. Besides its function in generating the active sites, the presence of the high concentration of ions in the ionic liquid is critical for the high conversion rate of the polyolefin at such low temperatures; it not only stabilizes carbenium ions as intermediates, thereby determining the overall reaction rate in the cracking-alkylation reaction, but also allows for easy separation of nonpolar alkane products from the reaction medium.

To visualize the conversion, experiments in glass-tube reactors using commercial low-density polyethylene (LDPE; weight-averaged molecular weight of ~4000, number-averaged molecular weight of ~1700) and iC_5 as substrates (the latter would be replaced by low–molecular weight, branched product alkanes in translation to a semicontinuous process) are shown as examples in Fig. 1. The Lewis acidic chloroaluminate ionic liquid consists of N-butylpyridinium chloride and anhydrous

$AlCl_3$ in a 1:2 molar ratio and is diluted in the present experiments in dichloromethane (denoted as $[C_4Py]Cl$-$AlCl_3$; see the materials and methods for details). The liquid catalyst, together with iC_5, led to complete LDPE conversion at 70°C after 3 hours in the presence of small amounts of $tert$-butyl chloride (TBC) to provide an initial concentration of carbenium ions to start the chain process. The yield of alkane products (C_4 to C_{36}) was twice as high as the amount of LDPE converted, reaching ~200 wt % (this suggests that, on average, an alkene with five C atoms is added relative to initial LDPE, and the stoichiometric mass ratio of LDPE/iC_5 was 1:1; see details in fig. S2); these products were present in the organic phase at the top, which was separated from the inorganic ionic liquid phase at the bottom. The main products were highly branched C_6 to C_{10} liquid alkanes (identified by gas chromatography–mass spectrometry in fig. S3), which accounted for ~126 wt % yield. Other products were gaseous isobutane (iC_4, ~48 wt %) and large alkanes (C_{11} to C_{36}, ~27 wt %). We found only traces of propane and propene (<0.1 wt %) in the headspace (fig. S4). The absence of methane and ethane allows us
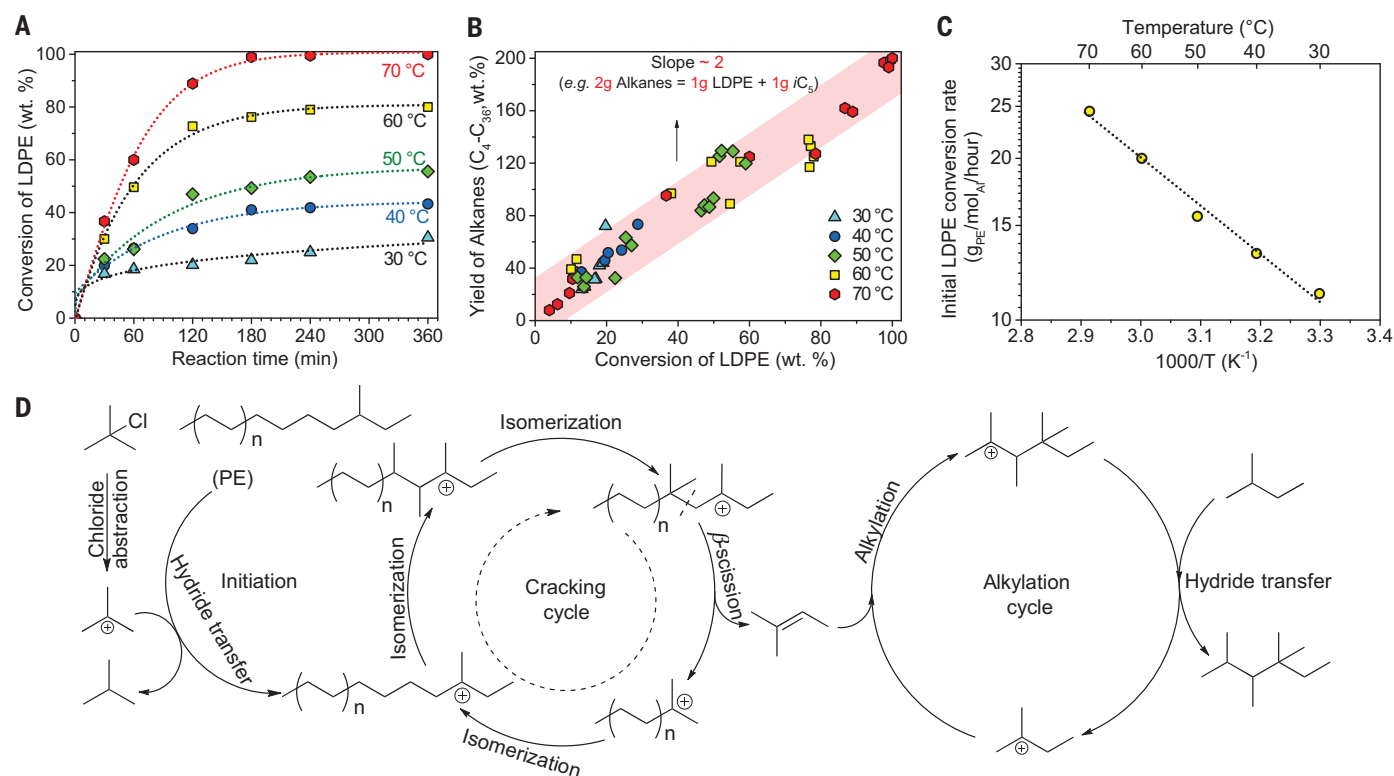

Fig. 2. Low-temperature catalytic performance for LDPE to alkanes and proposed reaction mechanism. (**A**) Time-resolved conversion profile of LDPE in the presence of TBC at different temperatures. Curves represent the optimal fit to the data, and all data were repeated at least five times and are shown as mean data points. (**B**) The corresponding mass yield to alkanes (C_4 to C_{36}) plotted against LDPE conversion. Reaction conditions were as follows: LDPE, 200 mg; iC_5, 800 mg; $[C_4Py]Cl$-$AlCl_3$, 3 mmol; TBC, 0.05 mmol; DCM, 3 ml; and temperature, 30° to 70°C. The red-shaded region represents a general linear fit to the data and is used to guide the eye. (**C**) Arrhenius plot for LDPE conversion with initial rates normalized to the aluminum content. (**D**) Proposed reaction mechanism for the tandem cracking-alkylation process of a polyolefin with iC_5. The 2-methyl-butene formed in the cracking cycle is depicted as an example that is based on the ratio of the molecular weight of the carbon products, which suggests that the ratio of converted LDPE and iC_5 is about 1:1 in the reaction, as deduced from Fig. 2B. PE, polyethylene.

to conclude that the reaction occurs overwhelmingly via carbenium ions and does not involve C–C cleavage via carbonium ions (figs. S5 and S6).

The control experiment with LDPE in the absence of iC_5 resulted in only 28 wt % LDPE conversion and produced a red-orange liquid with gaseous products that dominated the product distribution (~39 wt % isobutane and ~26 wt % pentane; see fig. S7). The yield of liquid alkanes in the range of C_6 to C_{10} was only 15 wt % (i.e., lower than the 61 wt % that was observed in the presence of iC_5), whereas the yield of large hydrocarbons (C_{11} to C_{36}) was as high as 20 wt %. In the absence of iC_5, olefinic hydrocarbons likely interact with the chloroaluminate anions, which deactivates the catalyst and yields adamantanes and acid-soluble conjunct polymers (so-called "red oil") (fig. S8) (25). In the presence of iC_5, alkanes were preferentially formed and accumulated in the iC_5-containing phase, separated in this way from the polar [ionic liquid with dichloromethane (DCM)] phase. Thus, iC_5 acts as an alkylating agent to form an alkane mixture, which resembles that of an isobutane or *n*-butene alkylation in the refining industry (24).

Because $[C_4Py]Cl$-$AlCl_3$ ionic liquid contains both Lewis and Brønsted acid sites (fig. S9A), the question arises whether the catalysis follows a reaction pathway that combines carbenium ion formation and sequential reactions catalyzed solely by Lewis acid sites or a reaction pathway that combines the carbonium ions formed by Brønsted acids with sequential reactions of carbenium ions (26). Carbenium ions are formed from alkanes at Lewis acid sites via hydride abstraction, whereas strong Brønsted acid sites form carbonium ions on the polymer strands that may crack or eliminate H_2 to form carbenium ions (27).

To discern the potential reaction pathways, we added co-reagents, including protic compounds [H_2O and CF_3COOH to generate carbonium ions (28)] and TBC [to generate carbenium ions (29)]. Adding protic co-reagents did not change the reaction rates or the product distribution compared with the reaction in their absence (see fig. S9B). Although traces of H_2 evolved, other products of protolytic cracking such as methane or ethane were completely absent. Thus, we rule out Brønsted acids and carbonium ions as the pathway to form carbenium ions. By contrast, adding TBC substantially enhanced the initial reaction rate by at least one order of magnitude and led to a nearly full conversion after 180 min, whereas only 20% was converted in its absence (fig. S9, B and C). The nature of the initiator did not markedly influence the rate of reaction (fig. S10, A and B). Control experiments using *n*-hexadecane as a model for LDPE reacting with iC_5 led to an identical enhancement (fig. S10, C and D). Thus, we

conclude that most of the carbenium ions are initiated via hydride abstraction from polymer strands by *tert*-butyl carbenium ions formed from TBC, with the reaction propagating via a carbenium ion chain mechanism (29). The high reaction rate is determined by the rate of polymer cracking via a carbenium ion chain mechanism, and the faster alkylation of intermediately formed alkenes with an isoalkane (eventually from the light fraction of the products) shifts the equilibrium such that full conversion is possible.

Temperature-dependent experiments (Fig. 2A) showed that the LDPE conversion increased from 20 to 90% after a 2-hour reaction time, when the reaction temperature was raised from 30° to 70°C. The yield of alkanes points to an overall single alkylation step, which leads to a yield of products that is approximately twice the mass of LDPE converted (Fig. 2B). In return, such an average product yield indicates that the average size of the intermediately formed alkene is close to pentene, followed by alkylation with iC_5 to yield decane isomers (fig. S11A). Actually, the main products are branched alkanes, with an average carbon number of ~8.4, which is lower than the theoretical value of 10. The lower carbon production represents higher H/C ratios, which means that the competing cyclization occurs and produces some polycyclic alkanes and acid-soluble oil with decreased H/C ratios. Evidently, the detected cyclohexanes and adamantanes as by-products (fig. S11B) agree well with this trend.

Figure 2C shows the logarithmic dependence of the initial rate of LDPE conversion on the

inverse temperature; from this, the apparent activation energy of the overall reaction was 17 ± 2 kJ/mol, which is much lower than the reported apparent activation barriers (163 to 303 kJ/mol) for the depolymerization of polyethylene so far (19). We also studied different isoalkanes using iC_4 and iC_6 as alkylating components for LDPE upcycling, which reached nearly 100 wt % of LDPE conversion and yielded branched alkanes (linear alkanes are negligible) under optimal conditions (fig. S12). This result demonstrates the practicability of recycling the lighter alkane product, that is, using iC_4 and iC_5 as the alkylation agents (details of recycling of light isoparaffins are given below).

To account for the tandem reaction proceeding with a constant rate, we posit two (independent) linked catalytic cycles based on carbenium ions, with cracking-derived alkenes serving as the linking intermediates (Fig. 2D). The fundamental differences in the reactivity dictate that in the initial stage of the reaction, hydride transfer from both the isoalkanes and the polyolefin dominates. As the reaction progresses, cracking of the polymer strands becomes predominantly associated with the cooperative action of alkylation. Thus, overall, the observed rates and product distributions are well explained by the two catalytic cycles depicted in Fig. 2D. The reaction is initiated by chloride abstraction from TBC. The formed carbenium ions abstract a hydride, preferentially from tertiary carbon atoms, both at branches in the polymer and in the more abundant iC_5. The carbenium ions formed in the polymer strands tend to undergo skeletal isomerization
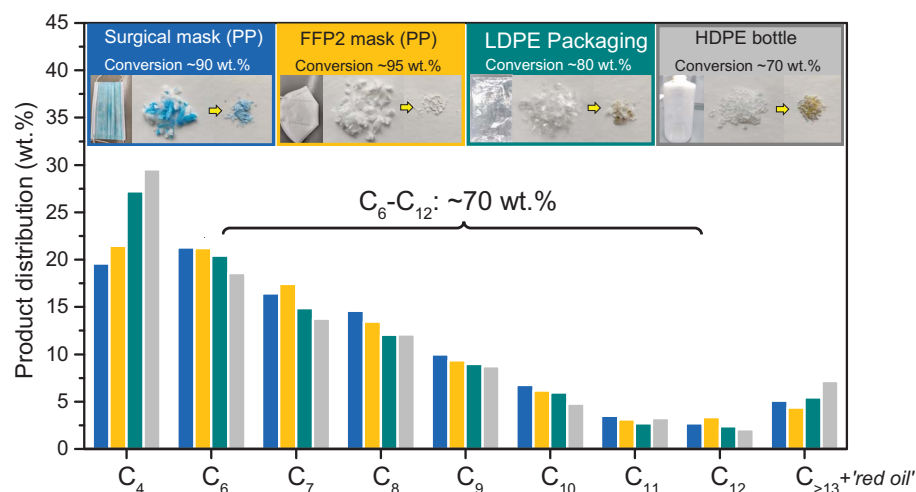
Fig. 3. Selective deconstruction of postconsumer polyolefin waste into liquid alkanes. Product distribution of tandem cracking-alkylation of postconsumer polyolefin waste with iC_5 with $[C_4Py]Cl$-$AlCl_3$. No methane, ethane, or propane was detected; all products were branched alkanes. Reaction conditions were as follows: polyolefin waste, 200 mg; iC_5, 800 mg; $[C_4Py]Cl$-$AlCl_3$, 3 mmol; TBC, 0.05 mmol; and DCM, 3 ml. Reaction temperatures and times were as follows: disposable surgical mask, 70°C for 6 hours; FFP2 mask, 70°C for 6 hours; food packaging, 70°C for 48 hours; and HDPE bottle, 100°C for 48 hours. PP, polypropylene; FFP, filtering face piece.
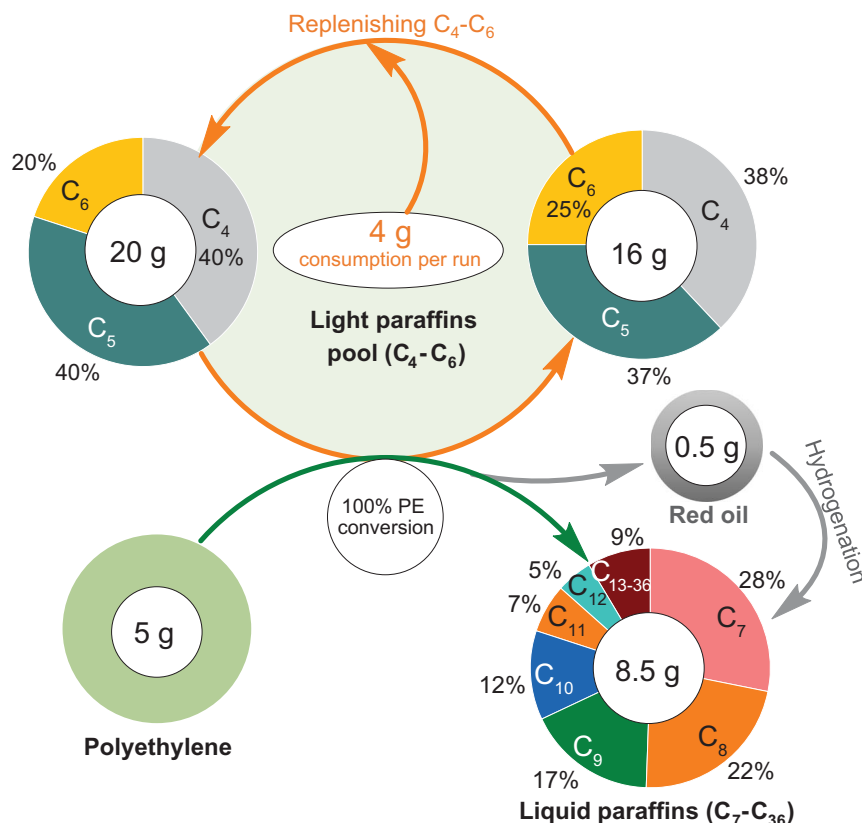
Fig. 4. Full conversion of polyethylene and isoparaffins that are recycled from the light products formed in the process. Cracking-alkylation of LDPE with light paraffin mixture (C_4 to C_6) as recycled light products from polyolefin deconstruction, which gives full LDPE conversion and branched C_{7+} alkanes. Each run only consumed 4 g of light paraffins from the pool, yielding 8.5 g of liquid isoparaffins (C_7 to C_{36}) and a minor amount of red oil as side products (0.5 g) that can easily hydrogenate to saturated hydrocarbons (fig. S20). Reaction conditions were as follows: LDPE, 5 g; initial light paraffin pool, 20 g (C_4, 40 wt %; C_5, 40 wt %; C_6, 20 wt %); [C_4Py]Cl-AlCl$_3$, 30 mmol; TBC, 100 mg; DCM, 75 ml; 2 MPa (N_2); temperature, 70°C; and reaction time, 2 hours.

and cracking via β-scission. Alkenes formed in this process (cracking cycle) react with carbenium ions formed from isoalkanes in the alkylation cycle. The detailed pathways using *n*-hexadecane as a model for LDPE are shown in figs. S13 and S14. The chemistry observed in this latter cycle is identical to that of the alkylation of isobutane with *n*-butene on such ionic liquid-based catalysts (*30*). Unless terminated by hydrogen transfer, these two cycles operate independently from each other, with their relative rates determining the product distribution. The rate of cracking in these coupled processes allows the use of an unusually low concentration of isoalkanes in the overall pool of reactive substrates compared with conventional isobutane and *n*-butene alkylation.

The final question to be addressed is the nature of the active sites that initiate and stabilize the chain propagation and catalysis that was observed. The speciation of [C_4Py]Cl-AlCl$_3$ ionic liquid depends closely on the initial ratio between *N*-butylpyridinium chloride and anhy-drous aluminum chloride, in which monomeric AlCl$_4^-$ and dimeric Al$_2$Cl$_7^-$ dominate at equilibrium (fig. S15). In situ ^{27}Al magic-angle spinning nuclear magnetic resonance spectroscopy (^{27}Al MAS NMR) and Raman spectroscopy showed that increasing the initial fraction of anhydrous aluminum chloride promotes the transformation from AlCl$_4^-$ to Al$_2$Cl$_7^-$, which in turn results in improved reaction rates (fig. S16). The observed catalytic behavior seems to be determined by the Lewis acidic Al$_2$Cl$_7^-$ anions (fig. S17), which were generally proposed as the catalytically active sites for catalysis over past decades (*31*). Intriguingly, further kinetic analysis uncovered that the reaction rate was not proportional to the concentration of Al$_2$Cl$_7^-$ (fig. S18) but rather to the transient aluminum trichloride (AlCl$_3$*) derived from the dissociation of Al$_2$Cl$_7^-$ (fig. S19). Unlike anhydrous aluminum chloride that features dimeric Al$_2$Cl$_6$, AlCl$_3$* species were undetectable and typically ignored because of the extremely small value of the equilibrium dissociation constant (*26*). To substantiate this inference, we plotted, in fig. S19, the turnover frequencies of [C_4Py]Cl-AlCl$_3$ against the concentration of AlCl$_3$*, which showed a linear correlation. Thus, we conclude that increasing the molar ratio of AlCl$_3$ to [C_4Py]Cl increases the concentration of dimeric Al$_2$Cl$_7^-$ species, which in turn results in an increased concentration of AlCl$_3$* active species.

The strategy described can near-quantitatively convert a wide selection of polymer consumer products with selectivity to C_6 to C_{12} products totaling more than 70 wt %, as exemplified by the results of reactions run using face masks, food packaging, and a high-density polyethylene (HDPE) bottle (Fig. 3). Depolymerization of HDPE bottles is less straightforward because of their compact structure, which lowers the contact surface or site between catalyst and granules, and will require further practical measures to increase dispersion. In practical implementation, the formed light isoalkanes (C_4 to C_6) can be recycled back as alkylating agents, which will ideally enable full conversion (because we hardly produce other light alkanes, including methane, ethane, and propane). To test this, we used the light isoparaffins mixture (C_4 to C_6) as the alkylating component for LDPE upcycling to simulate the recycling experiments, which reached full LDPE conversion and yielded branched alkanes (linear alkanes are negligible) (Fig. 4). Repeated batch experiments showed that the [C_4Py]Cl-AlCl$_3$ catalyst retained its activity and can be used at least five times without regeneration, thereby constantly reaching full LDPE conversion (fig. S20A). Some minor by-products, including red oil complexed with chloroaluminate anions, can be easily converted into saturated hydrocarbons via hydrogenation (fig. S20, B and C), which regenerates the [C_4Py]Cl-AlCl$_3$ ionic liquid. These results demonstrate the practicability of recycling the lighter alkane product as the alkylation agent. Although practical challenges will exist, scaling these results to a quasi-continuous process (conceptualized in fig. S21) is concluded to be highly promising and will integrate recycling of all light hydrocarbons or polymer swelling components.

Acidic chloroaluminate-based ionic liquids as emerging alkylation catalysts have already been industrially used in the paraffin alkylation process at Chevron's Salt Lake City refinery and China National Petroleum Corporation (CNPC), which demonstrates the stability of such catalysts (*32*). We thus envision that this upcycling strategy can be rapidly implemented not only in newly designed plants but also in existing refining technology. The synchronous release of alkenes via polyolefin cracking in the presented cascade cracking-alkylation conceptually allows for better control of product distribution and minimization of the formation of red oil waste (*27*), making polyolefins a

potential feed for refining alkylation. This work opens a transformative scalable approach to convert polyolefins and enables a critical contribution to a circular carbon economy.

REFERENCES AND NOTES

1. R. Geyer, J. R. Jambeck, K. L. Law, *Sci. Adv.* **3**, e1700782 (2017).
2. J. M. Garcia, M. L. Robertson, *Science* **358**, 870–872 (2017).
3. G. W. Coates, Y. D. Y. L. Getzler, *Nat. Rev. Mater.* **5**, 501–516 (2020).
4. S. C. Kosloski-Oh, Z. A. Wood, Y. Manjarrez, J. P. de Los Rios, M. E. Fieser, *Mater. Horiz.* **8**, 1084–1129 (2021).
5. Z. O. G. Schyns, M. P. Shaver, *Macromol. Rapid Commun.* **42**, e2000415 (2021).
6. S. M. Al-Salem, A. Antelava, A. Constantinou, G. Manos, A. Dutta, *J. Environ. Manage.* **197**, 177–198 (2017).
7. A. J. Martín, C. Mondelli, S. D. Jaydev, J. Pérez-Ramírez, *Chem* **7**, 1487–1533 (2021).
8. I. Vollmer et al., *Angew. Chem. Int. Ed.* **59**, 15402–15423 (2020).
9. L. O. Mark, M. C. Cendejas, I. Hermans, *ChemSusChem* **13**, 5808–5836 (2020).
10. G. Celik et al., *ACS Cent. Sci.* **5**, 1795–1803 (2019).
11. J. E. Rorrer, G. T. Beckham, Y. Román-Leshkov, *JACS Au* **1**, 8–12 (2020).
12. A. Tennakoon et al., *Nat. Catal.* **3**, 893–901 (2020).
13. S. Liu, P. A. Kots, B. C. Vance, A. Danielson, D. G. Vlachos, *Sci. Adv.* **7**, eabf8283 (2021).
14. X. Jia, C. Qin, T. Friedberger, Z. Guan, Z. Huang, *Sci. Adv.* **2**, e1501591 (2016).
15. N. Morlanés, S. G. Kavitake, D. C. Rosenfeld, J.-M. Basset, *ACS Catal.* **9**, 1274–1282 (2019).
16. F. Zhang et al., *Science* **370**, 437–441 (2020).
17. D. P. Serrano, J. Aguado, J. M. Escola, *ACS Catal.* **2**, 1924–1941 (2012).
18. H. Yan et al., *Science* **371**, 1257–1260 (2021).
19. L. D. Ellis et al., *Nat. Catal.* **4**, 539–556 (2021).
20. GlobalData, "Refinery alkylation units market installed capacity and capital expenditure (CapEx) forecast by region and countries including details of all active plants, planned and announced projects, 2022-2026," Report code GDGE1353ICR (2021).
21. A. Feller, I. Zuazo, A. Guzman, J. O. Barth, J. A. Lercher, *J. Catal.* **216**, 313–323 (2003).
22. N. Pfriem et al., *Science* **372**, 952–957 (2021).
23. L. Milaković, P. H. Hintermeier, Y. Liu, E. Baráth, J. A. Lercher, *Angew. Chem. Int. Ed.* **60**, 24806–24810 (2021).
24. H. K. C. Timken, S. Elomari, S. Trumbull, R. Cleverdon, "Integrated alkylation process using ionic liquid catalysts," US Patent 7,432,408 (2008).
25. C. J. Adams, M. J. Earle, K. R. Seddon, *Green Chem.* **2**, 21–24 (2000).
26. J. Estager, J. D. Holbrey, M. Swadźba-Kwaśny, *Chem. Soc. Rev.* **43**, 847–886 (2014).
27. A. Feller, J. A. Lercher, in *Advances in Catalysis*, H. Knüpffer, Ed. (Academic Press, 2004), vol. 48, pp. 229–295.
28. A. S. Amarasekara, *Chem. Rev.* **116**, 6133–6183 (2016).
29. S. Aschauer, L. Schilder, W. Korth, S. Fritschi, A. Jess, *Catal. Lett.* **141**, 1405–1419 (2011).
30. Y. Chauvin, A. Hirschauer, H. Olivier, *J. Mol. Catal.* **92**, 155–165 (1994).
31. R. Kore et al., *ACS Catal.* **7**, 7014–7028 (2017).
32. H. K. Timken, H. Luo, B.-K. Chang, E. Carter, M. Cole, in *Commercial Applications of Ionic Liquids*, M. B. Shiflett, Ed. (Springer, 2020), pp. 33–47.